Econ. Environ. Geol.
Vol. 29, No. 2, p. 129-138, 1996.

Characterization of Sericite Occurred in the Bobae Mine, Pusan, Korea

Ji-Won Moon* and Hi-Soo Moon*

ABSTRACT : **The ores of the Bobae mine are mainly composed of sericite and quartz, and with appreciable amount of some other minerals such as andalusite, pyrophyllite, and albite, etc.. Sericite occurs in various alteration zones having different crystal size and habit. Sericites can be classified into two types based on the crystal size; fine-grained and coarse-grained sericite. Fine-grained sericite occurs as an aggregate. Mineralogical characterizations of both types of sericites have been studied with various methods. Lattice parameters of two types of sericites occurred in various alteration zones are almost identical, but b parameter of coarse-grained sericite appears to be slightly bigger than that of fine-grained aggregates. Average structural formula of fine- and coarse-grained sericite is $K_{1.44}Al_{3.86}$ $(Si_{6.35}Al_{1.65})O_{20}(OH)_4$ and $K_{1.71}Al_{3.82}$ $(Si_{6.20}Al_{1.80})O_{20}(OH)_4$, respectively. Structural formulae of coarse-grained sericites are close to that of muscovite. Infrared spectra show that there is slight distinction between sericites occurred in andalusite-pyrophyllite zone and other subzones. IR spectra of sericites due to Si-O vibration (540~530 cm^{-1}) tend to shift to smaller wavenumber side from center to outer alteration zone. All samples have little or no interstratified minerals, and this is demonstrated by Ir and DTA-TG results. It indicates that the Bobae mine is formed at relatively high temperature. That the ratio of quartz to sericite in ores varies greatly indicates that several discontinuous hydrothermal alteration processes have been involved.**

INTRODUCTION

Intrusive igneous rocks are often associated both temporally and spatially with hydrothermal ore deposits such as many kinds of clay ore deposits. In the Bobae mine, several kinds of clay minerals such as sericite, pyrophyllite, chlorite, and smectite which were formed by the hydrothermal alteration occur in the Cretaceous rhyodacitic tuff of the Upper Yucheon Group.

Sericites have diverse mineral chemistry and structure (Hunziker *et al.*, 1986; Bishop, Bird, 1987; Eberl *et al.*, 1987; Spötl *et al*, 1993). Sericites ocurred in Korea have been studied by several workers during last few years such as the Daehyun mine (Rhee, 1991), Sangdong mine (Kim *et al.*, 1992) and Yukwang mine (Park *et al.*, 1992). A few investigations about the Bobae deposit have been done in terms of mineral chemistry and crystallographic study (Kim *et al.*, 1991; Hwang *et al.*, 1993), thermodynamic study (Choo, Kim, 1992), age dating about sericite ore minerals (Park *et al.*, 1992, 1993), and the occurrence and genetic environments by geochemistry and stable isotope study (Moon, Moon, 1995).

This study aims to identify the mineralogical characteristics of sericites occurred in the Bobae mine with various tools such as EPMA, XRD, DTA, TG, and IR.

GEOLOGIC SETTING AND ALTERATION ZONE

The Bobae sericite deposit occurs in rhyodacite of the Cretaceous Volcanogenic sedimentary rocks, Upper Yucheon Group, in the western part of Pusan (Chang, 1977). Detail geologic setting of the area and alteration zone of the Bobae mine were already reported by Kim *et al.* (1991), Hwang *et al.* (1993),

* Department of Geology, Yonsei University, 134 Shinchondong, Seoul 120-749, Korea

and Moon, Moon (1995). According to Moon, Moon (1995), the alteration zones can be divided into the phyllic and prophylitic zone based on the mineral assemblages. The phyllic zone is subdivided into three subzones; Andalusite-Pyrophyllite, Sericite and Albite subzones. Oxides vs. Al_2O_3 contents show variations corresponding to mineral assemblage in each alteration zone. According to Moon, Moon (1995), leaching of Ca, Na, and Mg and enriching of Si and K during the hydrothermal alteration process were observed. It was found that SiO_2 and K_2O increase in the Andalusite-Pyrophyllite subzone and Sericite subzone, respectively. These reflect variation of mineral assemblage. It closely related to alteration of parent minerals forming ore minerals.

Stable isotope data such as oxygen, hydrogen and sulfur isotope analysis indicate that the fluids were originally derived from the residual magmatic solution and have been mixed with abundant meteoric water later (Moon, Moon, 1995). The K-Ar ages of sericites indicate that the clay deposit is genetically related to the Hornblende-Biotite Granite which is also called by Masanite (Park, 1980) and Cretaceous~Paleocene Masan Hornblende-Biotite Granite (Lee, 1991).

SAMPLE AND METHODS

Ore samples were collected in the central gallery, open quarry face and altered zone around the mine on the basis of the degree of alteration. Those samples were powdered under 100 μm by tungsten carbide ball mill. Purified clay samples representing each alteration zone were prepared by sedimentation method.

Electron microprobe analyses have been done with a JEOL JXA-8600SX EDX model attached Si(Li) detector. Accelerating voltage of 15 kV, a beam current of 3.0 nA, 1~1.5 μm beam diameter, and an 100 second counting time were used. Well-characterized minerals were used for the standard minerals : quartz for Si, rutile for Ti, corundum for Al, hematite for Fe, rhodonite for Mn, periclase for Mg, wollastonite for Ca, jadite for Na, and sanidine for K. Data were corrected using the ZAF method.

XRD traces were obtained from untreated, ethylene glycol treated and heat treated orientation aggregates as well as random purified samples. MAC MXP-3 XRD system was used with Ni-filtered Cu-Kα radiation, 40 kV/30 mA, divergent and scattering slits of 1 mm, receiving slit of 0.15 mm, 0.02° 2θ steps, and counting times of 1 second per step. The shift of diffraction peak was calibrated by quartz sand to maintain accuracy and precision. Calculation of *hkl* and basal spacing is executed by using Lattice Constants Determination Program of above system.

The thermal behavior of the sample was investigated by Mac Science Co. TG-DTA 2000S system. Thermogravimetric analysis (TGA) and differnetial thermal analysis (DTA) were performed simultaneously in atmospheric condition at heating rate of 12℃/min and were obtained using Al_2O_3 as a reference material and Pt crucible. All specimens for the DTA were accurately prepared fine fractions and dried at 40℃ for one day prior to analysis.

Infrared (IR) spectra were obtained using FT Infrared Spectrometer for the clay fraction of representative sample in the frequancy range 300~400 cm^{-1}. Two mg of clay, which had been previously dried in oven at 100℃ and preserved in the desiccator containing $CaCl_2$ right before measuring to remove the adsorbed water, was mixed with 200 mg of KBr.

CHARACTERIZATION OF SERICITE

Mineral Composition of Sericite Ores

Sericite ores in the Bobae mine consist mainly of sericite with appreciable amounts of quartz and minor amounts of some other minerals such as andalusite, pyrophyllite, albite, pyrite, and interstratified mineral. Sericites occur as two types based on crystal habit and size; 1) sericite occurs as coarse sub/euhedral which has same habit like muscovite and 2) occurs as fine-grained aggregates which appear vein-shape or secondary sericite replaces other minerals formed in early stage including sub/euhedral sericite. However, the most common accessary mineral is quartz.

Table 1. X-ray powder diffraction data for sericite from the Bobae sericite mine.

PDF 26-991			BS-54			BS-1135			BS-205		
hkl	d	I/I_o	dcal	dobs	I/I_o	dcal	dobs	I/I_o	dcal	dobs	I/I_o
002	10.000	90	9.949	9.928	90	10.007	9.938	90	10.032	9.961	90
004	5.020	50	4.975	4.990	46	5.004	3.987	44	5.016	4.993	86
110	4.480	16	4.480	4.620	10	4.467	4.464	34	4.505	4.462	37
$\bar{1}11$	4.440	14	4.455	4.460	39	4.443			4.481		
$\bar{1}23$	3.590	8B	3.873	3.880	15	3.871	3.870	18	3.898	3.875	23
023	3.720	12	3.716	3.725	19	3.731	3.726	17	3.751	3.731	23
$\bar{1}14$	3.460	14B	3.484	3.483	32	3.486	3.482	30	3.508	3.493	40
006	3.340	100	3.344			3.336			3.344		
025	3.200	16	3.193	3.192	29	3.197	3.194	26	3.215	3.200	45
025	2.988	18B	2.977	2.992	27	2.991	2.991	29	3.004	2.990	51
115	2.867	12B	2.854	2.856	25	2.860	2.854	18	2.874	2.862	37
$\bar{1}16$	2.799	12	2.785	2.790	21	2.792	2.787	19	2.806	2.794	28
131	2.558	12B	2.551	2.555	42	2.554			2.572	2.561	53
008	2.509	8	2.487	2.496	15	2.502			2.508	2.497	27
$\bar{1}33$	2.463	8	2.475			2.458			2.475		
220	2.241	4	2.240			2.234			2.253		
136	2.005	50	1.993			1.999			2.009		
a= 5.19			a=5.197			a=5.172			a=5.220		
b= 9.00			b=8.975			b=9.002			b=9.061		
c=20.16			c=20.001			c=20.115			c=20.168		
β=95.18			β=95.799			β=95.747			β=95.799		
			V=928.104			V=931.763			V=948.895		

* I(intensity) values were recalculated to relative intensities by intensity of (002) peak as 90.

The ratio of quartz/sericite in sericite ore was determined by XRD method. The purified sericite and quartz from the ore were used for XRD work. The correction curve was obtained by average values of 3 measurements of each sample which has mixing ratio (sericite and quartz) from 90 : 10 to 10 : 90. For measuring peak intensity, the peak height (cps)×FWHM after extracting background by Sonneveld method (Sonneveld and Visser, 1975) was used instead of integrated area method. Because peaks are usually asymmetrical toward the low-angle direction and some of those have saddles. The method used in this study gives proportional errors in height or FWHM (Moore and Reynolds, 1989). Plots in Fig. 1 are the values of intensity ratio of quartz to sericite vs. quartz weight fraction by the previous calculated experimental correction curve equation, $X(SiO_2)=\ln (I_{ratio}/0.2649)/0.0593$. $X(SiO_2)$ is SiO_2 weight fraction to that of sericite, I_{ratio} is peak area of quartz (100) to peak area of sericite (002).

The $X(SiO_2)$ ranges 30~40 indicate that the active hydrothermal alteration reached equilibrium in those range and samples of the dispersed ranges indicate relic of climax of hydrothermal reaction, non-equilibrium state after crystallization and last stage of alteration.

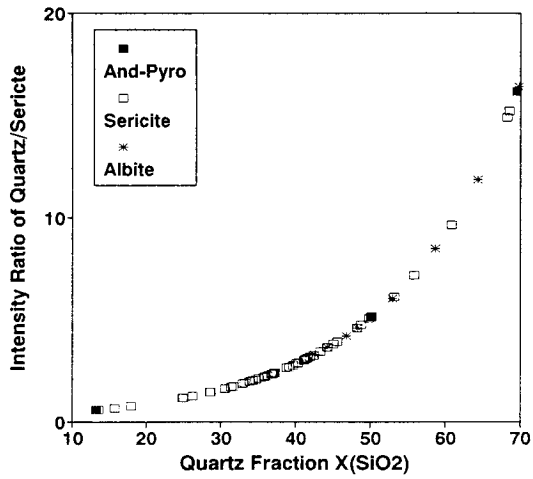

Fig. 1. Plots of $X(SiO_2)$ for ore samples of each zone projected on the correction curve.

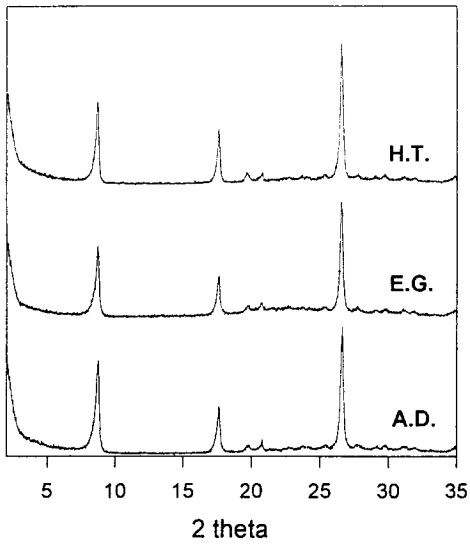

Fig. 2. X-ray diffraction patterns of representative purified sericite (CuKα radiation) : A.D.; air-dried, E. G.; ethylene-glycol treated, H.T.; heated at 550℃ for 1 hour.

Characterization by XRD

It is well known that only some diffraction peaks appear owing to preferred orientation of crystal. X-ray powder diffraction of some representative sericites was listed in Table 1. oriented samples shows (002), (004) and (006) diffraction peaks whereas randomly mounted samples show basal reflections with hkl reflections such as (110), ($\bar{1}$13), (023), ($\bar{1}$14), (114), (025), (115), (115), ($\bar{1}$16), and (131) peaks. Considering XRD patterns of representative sericites upon orientation, ethylene glycol, and heat treatment, they have little peak shifts or change of diffraction intensities (Fig. 2). It indicates that there is little or no interstratified layer in sericites.

XRD data show that the majorities of the samples are $2M_1$ polytype, They have strong (002), (006) peak and weak (004) peak with a few *hkl* reflections such as 3.88, 3.72, 3.49, 3.20, and 2.98Å peaks which are typical peaks of $2M_1$ polytype (Bailey, 1980). As shown in Table 1, the unit cell parameters of BS-54 (andalusite-pyrophyllite subzone), BS-1135 (sericite subzone), BS-205 (sub/euhedral coarse-grained sericite dominant samples) show variation. The unit cell dimensions are slightly bigger toward outward alteration zone. All of the calculated unit cell volumes are close to that of typical mucovite, 929Å^3, and these result is similar to 932.100~931.246Å^3 reported earlier by Choo (1989). But, especially sub/euhedral sericite is significantly bigger than that such as Rhee's result. 936.25~941.30Å^3 in the Daehyun Mine (Rhee, 1991).

Mineral Chemistry

Chemical analyses of representative sericites are given in Table 2. Two types of samples, fine- and coarse-grained sericites, were chosen for analysis for comparison.

Average structural formula of sub/euhedral and fine-grained aggreagates sericites is $K_{1.71}Al_{3.82}(Si_{6.20}\ Al_{1.80})O_{20}(OH)_4$ and $K_{1.44}Al_{3.86}(Si_{6.35}Al_{1.65})O_{20}(OH)_4$, respectively. K contents of coarse-grained sericite and fine-grained aggregates per unit cell are 1.66~1.77 and 1.26~1.64, respectively. The former is slightly larger than that of the later, but both are less than that of ideal muscovite. It is a general trends that Al substitutions increase as proceeding from tetrasilicic to trisilicic, therefore, Al in tetrahedral sites in sub/euhedral sericites (1.58~1.93) is higher than that of aggregates (1.52~1.81). Total cations in octahedral site of coarse-grained and fine-grained aggregates per unit cell value are 3.99~4.11 and 4.03~4.09. This result shows than the values of fine-grained sericites have narrower range than sub/euhedral coarse-grained sericites. Mineral chemistries of sericites show that some degree of relationship exists in terms of K contents between crystal habit, but on the contrary, there is no such a relationship between sericites occurred in different alteration zones.

All samples were plotted on MR^3-$2R^3$-$3R^2$ coordinates suggested by Velde (1985) in Fig. 3A. All plots are concentrated on the line MR^3-$2R^3$, and sub/euhedral sericites are slightly near the MR^3 vertex. Velde (1985) suggested that the plotted area in this diagram represent different geological environments. By this category, the fine-grained sericites plotted on the line MR^3-$2R^3$ indicate that those were formed by

Table 2. Electron microprobe analyses and structure formulae for sericite.

Sample	1114			26		1148	4		■
Name	2-5	2-3	2-4	2-6	3-4	1-1	1-1	2-2	Ave.
SiO_2	45.15	45.42	45.02	45.11	44.96	45.77	47.68	46.53	45.70
TiO_2	0.28	0.13	0.08	0.12	0.62	0.80	0.72	0.11	0.36
Al_2O_3	34.36	36.05	37.37	36.79	36.29	32.93	33.28	33.84	35.11
FeO*	1.73	0.32	0.28	0.10	0.34	1.97	0.31	1.53	0.82
MnO	0.08	0.06	0.06	0.00	0.00	0.13	0.00	0.00	0.04
MgO	0.70	0.18	0.00	0.00	0.00	0.18	0.89	1.17	0.51
CaO	0.06	0.08	0.00	0.00	0.02	0.02	0.00	0.00	0.02
Na_2O	0.41	0.29	0.26	0.37	0.44	0.28	0.28	0.22	0.32
K_2O	10.12	9.63	9.91	10.17	9.60	9.97	9.77	9.99	9.90
Total	92.89	92.14	92.98	92.66	92.27	93.04	92.93	93.38	92.79
				Numbers of ions on the basis of 22 oxygen					
Si	6.17	6.17	6.07	6.11	6.11	6.25	6.42	6.29	6.20
Al	1.83	1.83	1.93	1.89	1.89	1.75	1.58	1.71	1.80
Al(VI)	3.71	3.95	4.01	3.99	3.92	3.55	3.70	3.69	3.82
Ti	0.03	0.01	0.01	0.01	0.06	0.08	0.07	0.01	0.04
Fe	0.20	0.04	0.03	0.01	0.04	0.22	0.03	0.17	0.09
Mn	0.01	0.01	0.01	0.00	0.00	0.01	0.00	0.00	0.00
Mg	0.14	0.04	0.00	0.00	0.00	0.24	0.18	0.24	0.10
ΣVI(IV)	4.09	4.04	4.06	4.01	4.03	4.11	3.99	4.11	4.05
Ca	0.01	0.01	0.00	0.00	0.00	0.00	0.00	0.00	0.00
Na	0.11	0.08	0.07	0.10	0.12	0.08	0.07	0.06	0.08
K	1.77	1.67	1.71	1.76	1.66	1.74	1.68	1.72	1.71

Sample	54			26		1148		1110	□
Name	3	5	1-1	1-2	2-5	3-4	3-5	2-1	Ave.
SiO_2	49.31	46.47	48.14	47.80	46.62	47.37	46.03	49.97	47.71
TiO_2	0.06	0.00	1.07	1.22	0.04	0.16	0.10	0.00	0.33
Al_2O_3	37.07	36.39	32.60	31.83	36.86	34.05	35.92	36.25	35.14
FeO*	0.08	0.26	0.65	0.63	0.14	1.04	1.08	0.29	0.52
MnO	0.00	0.08	0.00	0.02	0.04	0.07	0.00	0.00	0.03
MgO	0.00	0.00	1.60	2.19	0.00	0.25	0.28	0.00	0.54
CaO	0.03	0.09	0.00	0.00	0.09	0.91	1.04	0.18	0.29
Na_2O	0.26	0.24	0.11	0.23	0.30	0.52	0.75	0.14	0.32
K_2O	8.16	8.89	9.58	9.58	9.23	7.27	7.51	7.78	8.50
Total	94.96	92.51	92.75	93.32	93.32	91.65	92.69	94.61	93.37
				Numbers of ions on the basis of 22 oxygen					
Si	6.39	6.24	6.43	6.42	6.22	6.41	6.19	6.48	6.35
Al	1.61	1.76	1.57	1.58	1.78	1.59	1.81	1.52	1.65
Al(VI)	4.05	4.02	3.57	3.45	4.02	3.84	3.88	4.03	3.86
Ti	0.01	0.00	0.11	0.12	0.00	0.02	0.01	0.00	0.03
Fe	0.01	0.03	0.07	0.07	0.02	0.12	0.12	0.03	0.06
Mn	0.00	0.01	0.00	0.00	0.00	0.01	0.00	0.00	0.00
Mg	0.00	0.00	0.32	0.44	0.00	0.05	0.06	0.00	0.11
ΣVI(IV)	4.06	4.06	4.06	4.09	4.04	4.03	4.07	4.06	4.06
Ca	0.00	0.01	0.00	0.00	0.01	0.13	0.15	0.02	0.04
Na	0.06	0.06	0.03	0.06	0.08	0.14	0.19	0.03	0.08
K	1.35	1.52	1.63	1.64	1.57	1.26	1.29	1.29	1.44

* Fe total as FeO, ■; Average value of coarse-grained sericites, □; Average value of fine-grained aggregates.

hydrothermal alteration processes, and some of sub/euhedral coarse-grained sericite plotted near the MR[3] vertex appear to be magmatic micas. These results show a reasonably good agreement with that was

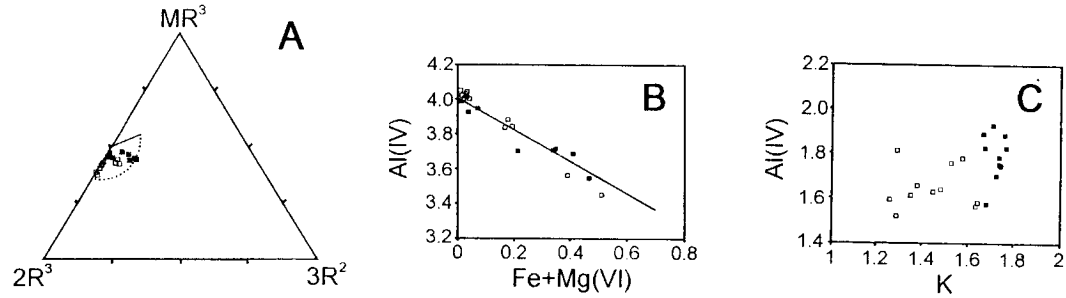

Fig. 3. Chemical relationships among sericites in altered rocks. A) plots of sericite compositions in MR^3-$2R^3$-$3R^2$ coordinates near muscovite composition. B) plots of Al^{VI} against (Fe+Mg) in octahedral sites. C) Plots of Al^{IV} against K (solid square; coarse-grained sericites, open square; fine-grained sericites).

reported by earlier workers (Kim *et al.*, 1991; Moon , Moon, 1995). They concluded that both types of sericites were originated from replacement and reprecipitation during hydrothermal alteration with fluid related to magmatic sources.

Sericites deplete Al contents in the octahedral site and K in the interlayer comparing with ideal composition of muscovite, whereas enrich Si in the tetrahdral site. The chemical composition shows that substitution Si^{4+} for Al^{3+} causes increasing divalent octahedral cations like Fe^{2+} or Mg^{2+} to match total layer charge. There is a negative relationship between Fe+Mg and Al in octahedral sites as shown in Fig. 3B, whereas weak positive relationship between K in the interlayer and Al^{3+} in octahedral can be observed (responsible for charge compensation) as shown in Fig. 3C. Obvious difference in K contents between two types of sericites can be monitored, but this kind of relationship does not hold for sericites occurred in various alteration zones.

Expandability of Sericite

Commonly interstratified minerals can be found alteration zones of hydrothermal ore deposit. Kim *et al.* (1991) and Hwang *et al.* (1993) reported that ores of the Bobae mine have no or little interstratified minerals. Eberl *et al.* (1987) stated that traces of expandability can be detected by using Ir (intensity ratio, $(I(001)/I(003))/(I(001)/I(003))_{E.G.}$ introduced by Ś rodoń *et al.* (1984). Therefore, Ir was measured in order to confirm presence of expandable layer.

Table 3. XRD data for sericite from the Bobae mine.

Alteration zone	Sample name	d(002)	Ir	Kubler index
Andalusite-Pyrophyllite	BS-54	10.1092	1.08	2.0
	BS-1155	10.0858	1.13	2.0
	BS-26	10.1092	1.04	1.8
	BS-52	10.0402	1.18	2.0
	Average		1.11	1.95
Sericite	BS-1099	10.1554	1.01	2.0
	BS-1135	10.0513	1.18	2.3
	BS-1050	10.0858	1.03	2.0
	BS-1118	10.1554	1.00	1.8
	Average		1.06	2.02
Albite	BS-1068	10.0858	0.80	1.8
	BS-1112	10.1092	1.11	1.8
	Average		0.96	1.80

Purified clay size fractions of the Bobae mine contain micro quartz (Kim *et al.*, 1991; Hwang *et al.*, 1993; Moon, Moon, 1995). It causes a severe problem for Ir calculation because 3.32Å peak of sericite is overlapped by 3.34Å peak of quartz. Therfore, 5.02Å peak of sericite was used for Ir calculation in this study. Although exactly same weight (30 mg) of clays was mounted, it is virtually impossible for all samples to stack and to be diffracted in the same condition. Average values of Ir using (002) and (004) peak are listed in Table 3. Ir of sericite from various alteration zones is as follows, andalusite-pyrophyllite subzone, 1.11, sericite subzone, 1.06; and albite subzone, 0.96. This result is similar to that of Kim *et al.* (1991). indicating that there is little possibility of existence of interstratified minerals in the examined samples. In comparision with the result of Eberl *et al.*

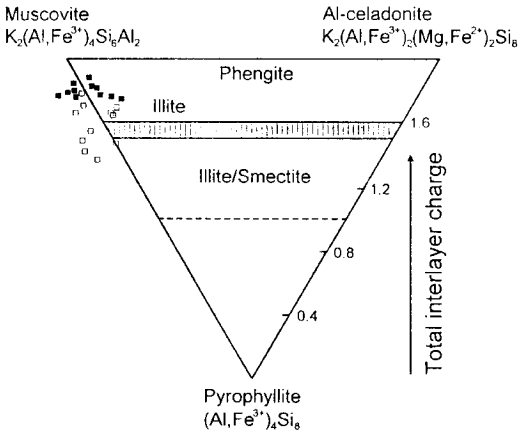

Fig. 4. Dioctahedral 2 : 1 layer silicates with Fe<1 per O_{20} $(OH)_4$ projected on a triangle have three corner (muscovite, Al-celadonite, pyrophyllite) of a prism face (after Yoder and Eugster, 1955; Newman and Brown, 1987). Shading indicates a range of charge betwenn illite *sensu stricto* (<5% expanding layers) and illite-smectite. Symbols are the same as used in Fig. 3.

(1987), Ir values of all samples lie between 1.00~1.18 except for BS-1068 (of which peak is interfered by small amount of smectite). It suggests that these samples have interstratified minerals less than 3%. The Kubler indices of the samples (1.8~2.3) as shown in Table 3 indicate that they have interstratified minerals less than around 3.6%.

Fig. 4 illustrates the possibility of existence of interstratified minerals by octahedral, tetrahedral and interlayer charge using micriprobe analyses data (Yoder, Eugster, 1955). Both sub/euhedral coarse-grained and fine-grained aggregate sericite were plotted in the area of hydrous mica except some fine-grained aggregates which have more or less 5% expandable layers. Plots out of the muscovite, Al celadonite, and pyrophyllite coordinate were caused by several reasons. The errors might be due to the calculation of structural formula, the presence of impurities in fine-grained aggregates or analysis error itself. Analysis error is probably main cause lead such a result because beam diameter is bigger than that of individual particle size for fine-grained aggregates. However, this result also confirms that there is no or little interstratified minerals in the samples of the Bobae mine.

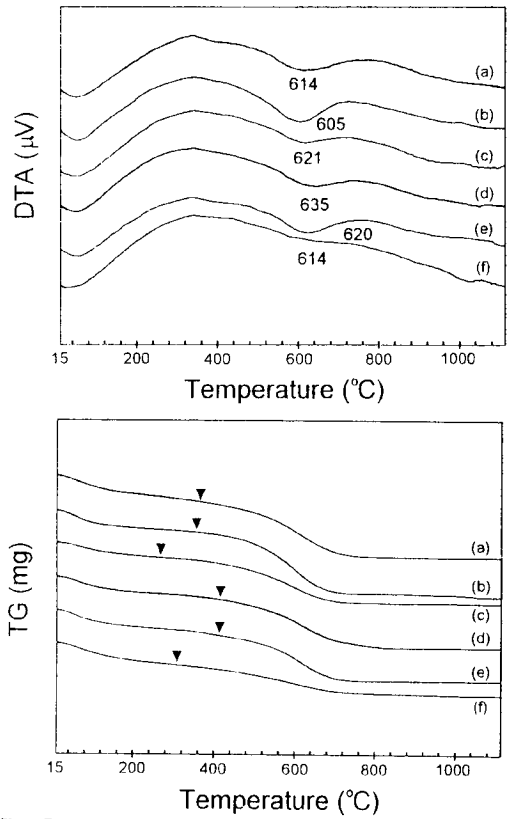

Fig. 5. DTA-TG curves for representative purified sericits of each zone. (a) BS-205, (b) BS-52, (c) BS-54, (d) BS-1099, (e) BS-1135, and (f) BS-1112.

Thermal Property

DTA and TG curves are plotted in Fig. 5 for the representative sericite samples of each zone. BS-205 is a sub/euhedral sericite. BS-52 and BS-54 are collected from andalusite-pyrophyllite subzone; BS-1099 and BS-1135 are from sericite subzone and BS-1112 is from albite subzone. As mentioned before, mineral chemistry of these sericites differ from muscovite in several ways. Sericite contains less silicon. Consequently, SiO_2/Al_2O_3 ratio is reduced and thus the excess negative charge is reduced. This fact explains why the K ions are partially replaced with other cations and decreasing K_2O causes that the amount of adsorbed water would increase. But, in Fig. 5, sericites show a small endothermic peak at low temperature below 100℃ due to the removal of the

Table 4.Weight loss (%) of representative sericite samples by TG.

Sample name	Tot. wt. (mg)	X(SiO_2)	Sericite wt. (mg)	Dehydration		Dehydroxylation		Tot. Wt. loss(%)
				(mg)	(%)	(mg)	(%)	
BS-205	24.1	0.000	24.100	0.462	1.92	1.000	4.15	6.07
BS-52	27.2	32.738	18.295	0.389	2.12	1.150	6.29	8.41
BS-54	25.9	2.366	25.287	0.250	0.99	0.840	3.32	4.31
BS-1099	24.8	21.077	19.573	0.448	2.29	0.892	4.55	6.85
BS-1112	22.3	17.021	18.504	0.398	2.15	0.562	3.03	5.18
BS-1135	24.7	26.300	18.204	0.463	2.54	0.567	3.12	5.66

adsorbed water. The second endothermic peak at 604~634℃ is due to dehydroxylation and these temperatures are distingusished with that of muscovite. That the expulsion of hydroxyl groups take place between 750~950℃ in muscovite, which cause a broad endothermic effect to appear on the thermal curves. It indicates that the bond energy of hydroxyl in sericite is samaller than that in muscovite. On the basis of TG curves, it is possible to establish how the mass of the sample varies under the influence of thermal energy. The total weight weight loss in sericite is measured and the results are listed in Table 4. Weight loss is continued up to 1,000℃. Considering DTA curves of the samples, there is no evidence for illite-montmorillonite interstratified minerals. Because two endothermic reaction in the mid-temperature region for typical montmorillonites can not be observed (Mackenzie, 1970) and only one endothermic peak of sericite is detected.

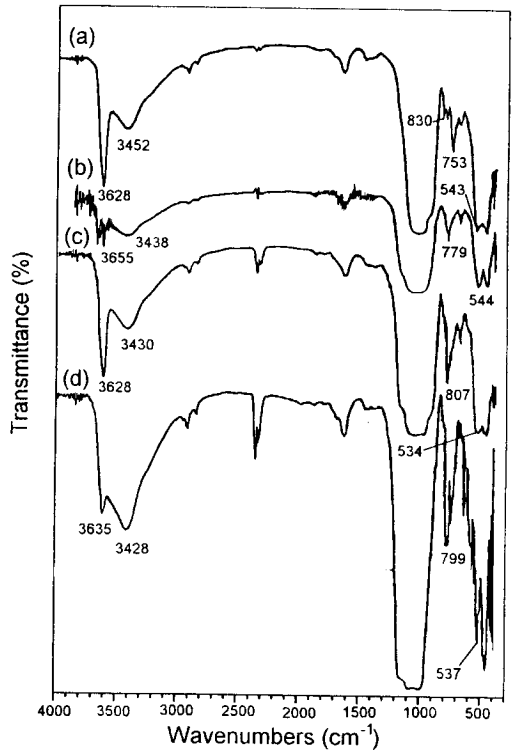

Fig. 6. IR srectra for representative purified sericites of each zone.

Infrared Spectroscopy

Sericite has generally the broad band due to O-H bond vibration near 3,625 cm^{-1}, coupled with the 825, 750 cm^{-1} doublet (Wison, 1987). Fig. 6 shows IR spectra of representative sericite samples for sub/euhedral and each alteration subzone. All the spectra are characteristic of dioctahedral, aluminous clay minerals that are similar in composition to muscovite (Veld. 1978) such as absorption bands near 3,625 cm^{-1} by O-H vibration and near 1,030 cm^{-1} by Si-O vibration. They do not have bands near 3,260 and 1,430 cm^{-1} which indicate interlayer NH^{4+} ions replacing K^{+} during diagenesis. However, only sub/euhedral sericite has 830 and 753 cm^{-1} peak and others have 779~807 cm^{-1} peak between two peaks. Those two peaks are characteristic absorption band of muscovite-like sericite, and other samples without these peaks belong to phengite-like type.

There is a close relationship between mineral chemistry and infrared spectra. Fig. 6 also indicates an approximate correlation between the sericite composition (Table 2.) and IR spectra. Subtle change

on the spectra is accompanied by an increase in the depth of the valley between 915 and 830 cm^{-1} band and shift of the Si-O bond vibration between 540~530 cm^{-1}. Such a variations are due to the amount of octahedral Fe+Mg (Stubican, Roy, 1961; Hunziker *et al.*, 1986; Eberl *et al.*, 1987). Si-O bond vibration bands of (a) sub/euhedral, 543 cm^{-1} and (b) andalusite-pyrophyllite subzone, 544 cm^{-1} tend to shift to small wavenumber direction such as (c) sericite subzone, 534 cm^{-1} and (d) albite subzone, 537 cm^{-1}.

Andalusite-pyrophyllite subzone is the most intensive altered zone and is a place to give a circumstance in which sub/euhedral sericites grow. This result is supported by the fact that average amount of FeO+MgO of sub/enhedral sericite is 1.79 contrary to 1.51 of fine-grained aggregates and octahedral Fe+Mg equivalents per $O_{10}(OH)_2$ is 2.7 contrary to 2.4 in Table 2.

DISCUSSION AND CONCLUSION

Sericites occur as ore mineral which appears in all altered zone. These sericites can be grouped into two types based on crystal habit and size; fine-grained aggregates and coarse-grained sub/euhedral sericite. The average structural formula of the former and the latter is $K_{1.44}Al_{3.86}(Si_{6.35}\ Al_{1.65})O_{20}(OH)_4$ and $K_{1.71}\ Al_{3.82}\ (Si_{6.20}A_{1.80})O_{20}(OH)_4$ respectively. The structural formula of coarse-grained sericite is more close to that of ideal muscovite. K contents of coarse-grained sericite and fine-grained aggregates per unit cell are 1. 66~1.77 and 1.26~1.64, respectively. The former is slightly larger than that of the later, both are less than that of ideal muscovite. Sericites show that some degree of relationship exists in terms of K contents between crystal habit, but on the contrary, there is no such a relationship between sericites occurred in different alteration zones.

XRD data shows that the majorities of the samples are $2M_1$ polytype (Bailey, 1980). The calculated unit cell volumes range 932.100~931.246 $Å^3$ which is close to that of typical muscovite, 929 $Å^3$. It was noted that unit cell dimensions are slightly bigger toward outward alteration zone. All sericites occurred in the mine have little or no interstratified minerals except for chlorite/smectite as a weathering product of basic vein (Hwang, 1993). This is confirmed by measured Ir (intensity ratio) and DTA-TG result. This means that the Bobae sericite mine is formed at relatively high temperature.

Sericites which occur in different alteration zones and have different habit were examined by XRD, DTA, TG, and IR. Those results reveal that there is not distinct differences between sericites occurred in each different alteration zone. This means that all of sericites were formed identical genetic environments regardless crystal habit. From the ratio of quartz to sericite, their wide range of variation indicate that irregular and partial reactions continued after main hydrothermal alteration.

ACKNOWLEDGMENT

This study was supported by the Center for Mineral Resources Research sponsored by the Korea Science and Engineering Foundation.

REFERENCES

Bailey, S. W. (1980) Summary of recommendation of AIPEA nomenclature committee, Clay Minerals, Vol. 15, p.85-93.

Bishop, B. P. and Bird, D. (1987) Variation in sericite compositions from fracture zones within the Coso Hot Springs geothermal system. Geochim. Cosmochim. Acta, V.51, p.1245-1256.

Chang, K. H. (1977) Late Mesozoic stratigraphy, sedimentation and tectonics of southeastern Korea. Jour. Geo. Soc. Korea, 13, 76-90 (in Korean).

Choo, C. O. (1989) Mineralogy of clay minerals from Bobae-Kimhae mines, Kimhae, Korea. M. S. Thesis, Seoul National University, 74p.

Choo, C. O. and Kim, S. J. (1992) Formation of illite in the natural K_2O-Al_2O_3-SiO_2-H_2O system in the hydrothermal clay deposit of the Bobae mine, Korea. J. Miner. Soç. Korea, 5, 6-13.

Eberl, D. D. Srodoń, J., Lee, M., Nadeau, P. H and Northop H. R. (1987) Sericite from the Silverton caldera Colorado : Correlation among structure, composition, origin, and particle thickness, Amer, Miner. 72, 914-934.

Hunziker, J. C., Frey, M., Clauer, N., Dallmeyer, R. D. Friedrichsen, H., Flehming, W., Hochstrasser, K., Roggwiler, P., and Sohwander, H. (1986) The Flehming, evolution of illite to muscovite : Mineralogical and isotopic data from the Glarus Alps.

Switzerland. Contrib. Miner. Petrol., 92, 157-180.
Hwang, J. Y., Kim, K. H., and Jeong, Y. Y. (1993) Occurrence of clay minerals from the Bobae pottery stone mine in Pusan. J. Miner. Soc. Koera, 6, 27-37 (in Korean).
Kim, J. D., Moon, H. S., Jin, S. J., and Kim, I. J. (1992) Mineral chemistry and stable isotope composition of sericite from the Sangdong sericite mine in the Kimhae area. Jour. Korea Inst. Min. Geol., 25, 275-282 (in Korean).
Kim S. J., Choo, C. O., Park. H. I. and Noh, J. H. (1991) Mineralogy and genesis of hydrothermal deposits in the Southeastern part of Korea Peninsula : (2) Bobae sericite seposits, Jour. Miner. Soc. Korea, 4, 129-140.
Lee, J. I. (1991) Petrology, mineralogy and isotopic study of the shallow-depth implaced granitic rocks, southern part of the Kyoungsang Basin, Korea : Origin of micriographic granite. D.S. Thesis, University of Tokyo, 197p.
Mackenzie, R. C. (1970) Differnetial thermal analysis, Vol 1, Fundamental Aspects, Academic press, London.
Moon, J. W. and Moon, H. S. (1995) Occurrences and genetic environment of the Bobae sericite deposit, Pusan area, Econ. Environ. Geol., 28, 93-107 (in Korean).
Moore, D .M. and Reynolds, Jr., R. C. (1989) X-ray diffraction and the identification and analysis of clay minerals. ed. Oxford University Press, Oxford, New York, P.332.
Park, B. Y. (1980) Granites in Masan area with special reference to their chemical variations. Jour. Geol. Korea, 16, 135-148.
Park, H. I., Chang, H. W., and Moon, H. S. (1992) Ore-forming mechanisms and divisions in the Kyungsang basin, Korea. Objective basic research 1 st term (1992) report, KOSEF (in Korea).
Park, H. I., Chang, H. W., and Moon, H. S. (1993) Ore-forming mehanisms and divisions in the Kyungsang basin, Korea. Objective basic research 2 st term (1993) report, KOSEF (in Korean).
Park, M. E., Choi, I. S., and Kim, J. S. (1992) Hydrothermal solution-rhyolite reaction and origin of sericite in the Yukwang mine. Korea Inst. Min. Geol., 25, 225-232 (in Korean).
Rhee, B. Y. (1991) Mineralogy of sericites in the Daehyun mine, Korea. Ph. D. Thesis, Seoul National University.
Russell, J. D. (1974) Instrumentation and techniques. In the infrared spectra of minerals. Farmer, V. C. ed/ London : Mineralogical Society, P. 11-25.
Sonneveld, E. J. and Visser, J. W. (1975) Automatic collection of powder data from photographs. J. Appl. Cryst., 8, 1-7.
Spötl, C., Houseknecht, D. W., and Jaques, R. (1993) Clay mineralogy and illite crystallinity of the Atoka formation, Arkoma basin, and Frontal Ouachita mountains., Clays Clay Miner., v.41, P.745-754.
Środoń, J. and Eberl, D. D. (1984) Illite : in micas, S. W. Bailey, ed., Reviews in Minralogy 13, Mineralogical society of America, Washington, D. C., 495-544.
Stubican, V. and Roy, R. (1961) Isomorphous substitution and the infrared spectra of layer lattice silicates. Amer. Miner., 46, 32-51.
Todor, D. N. (1976) Thermal analysis of minerals. ed. Abacus Press, Tunbridge Wells, England.
Velde, B. (1978) Infrared spectra of synthetic micas in the series muscovite-MgAl celadonite. Amer. Miner., 263, 886-913.
Velde, B. (1985) Clay minerals : A physico-chemical explanation of their occurrence. ed. Elselvier Science Publishing Company Inc., New York.
Wilson, M. J. (1987) A handbook of determinative method in clay mineralogy. ed. Blackie & Son Ltd, London.
Yoder, H. S. and Eugster H. P. (1955) Synthetic and natural muscovite. Geochim. cosmochim. Acta, 6, 157-185.

Manuscript received 9 March 1996

부산 보배광산산 견운모의 광물학적 특성

문지원 · 문희수

요 약 : 보배광산의 광석광물은 주로 석영과 견운모로 구성되어 있다. 견운모는 이 광상의 각 변질대에서 산출되나, 그 정상에 의하여 조립질과 세립질로 구분된다. 각 변질대별 대표시료에 대한 결정광학적 특징은 유사하며, 단지 조립질 견운모의 경우 세립질 보다 b* 값이 약간 크다. 세립질 및 조립질 견운모의 평균구조식은 $K_{1.44}Al_{3.86}(Si_{6.35}Al_{1.65})O_{20}(OH)_4$과 $K_{1.71}Al_{3.82}(Si_{6.20}Al_{1.80})O_{20}(OH)_4$이며 조립질의 경우 백운모의 조성에 더욱 가깝다. 본 광산의 견운모는 혼합층광물을 거의 함유하지 않으며(5% 미만), 이는 Ir와 DTA-TG 결과로 확인된다. 적외선흡광분석결과, 홍주석-납석대에서 산출되는 견운모의 540~530 cm^{-1} 영역의 Si-O 진동이 변질대 외곽에서 산출되는 견운모로 갈수록 낮은 진동수 쪽으로 이동하는 특징을 보인다. 변질대간 광석광물의 특징이 확실히 구별되지 않는 것은 은미정질 견운모가 기존에 고온에서 형성된 완정질 견운모를 치환하기 때문이며, 이는 석영 : 견운모간 몰비를 통해서도 알 수 있다. 두 광물의 존재비가 넓은 분포를 보이는 것은 변질의 정점을 지난 불규칙적이고 부분적인 반응이 계속 일어났음을 의미한다.